Light-Induced Structural Changes in a Putative Blue-Light Receptor with a Novel FAD Binding Fold Sensor of Blue-Light Using FAD (BLUF); Slr1694 of *Synechocystis* sp. PCC6803[†]

Shinji Masuda,[‡] Koji Hasegawa,[‡] Asako Ishii, and Taka-aki Ono*

Laboratory for Photo-Biology (1), RIKEN Photodynamics Research Center, The Institute of Physical and Chemical Research, 519-1399 Aoba, Aramaki, Aoba, Sendai 980-0845, Japan

Received January 22, 2004; Revised Manuscript Received March 3, 2004

ABSTRACT: The sensor of blue-light using FAD (BLUF) domain is the flavin-binding fold categorized to a new class of blue-light sensing domain found in AppA from *Rhodobacter sphaeroides* and PAC from *Euglena gracilis*, but little is known concerning the mechanism of blue-light perception. An open reading frame *slr1694* in a cyanobacterium *Synechocystis* sp. PCC6803 encodes a protein possessing the BLUF domain. Here, a full-length Slr1694 protein retaining FAD was expressed and purified and found to be present as an oligomeric form (trimer or tetramer). Using the purified Slr1694, spectroscopic properties of Slr1694 were characterized. Slr1694 was found to show the same red-shift of flavin absorption and quenching of flavin fluorescence by illumination as those of AppA. These changes reversed in the dark although the rate of dark state regeneration was much faster in Slr1694 than AppA, indicating that Slr1694 is a blue-light receptor based on BLUF with the similar photocycle to that of AppA. The dark decay in D_2O was nearly four times slower than in H_2O. Light-induced Fourier transform infrared (FTIR) difference spectroscopy was applied to examine the light-induced structure change of a chromophore and apo-protein with deuteration and universal ^{13}C and ^{15}N isotope labeling. The FTIR results indicate that light excitation induced distinct changes in the amide I modes of peptide backbone but relatively limited changes in flavin chromophore. Light excitation predominantly weakened the C(4)═O and C(2)═O bonding and strengthened the N1C10a and/or C4aN5 bonding, indicating formational changes of the isoalloxazine ring II and III of FAD but little formational change in the isoalloxazine ring I. The photocycle of the BLUF is unique in the sense that light excitation leads to the structural rearrangements of the protein moieties coupled with a minimum formational change of the chromophore.

Various types of blue-light receptors that use the flavin chromophore are distributed in species ranging from prokaryotes to eukaryotes and are involved in numbers of biological events, which are controlled by blue-light. Recent studies have indicated that there are three classes of flavin-binding domains in flavin-containing blue-light receptors (reviewed in refs *1*−*5*). One is the flavin mononucleotide-binding LOV[1] domain of plant phototropins (phot1 and phot2) that mediate the blue-light signal for regulating diverse physiological response to blue-light, including phototropism, chloroplast relocation, and stomatal opening. The second class is the FAD-binding domain of plant cryptochromes that are involved in hypocotyls cell elongation, cotyledon/leaf expansion, petiol/flower elongation, and circadian rhythm. Cryptochrome also functions for the phasing of the circadian clock in *Drosophila* and mice. The third class was exemplified most recently in AppA (*6*) and PAC (*7*).

The AppA protein in the purple bacterium *Rhodobacter sphaeroides* interacts with a photosynthesis repressor PpsR to form a stable AppA−$(PpsR)_2$ complex in the dark and in low-light conditions. Blue-light activated AppA cannot associate with PpsR and, therefore, enables PpsR to bind to various promoters of the photosynthetic genes and inhibit the transcription (*6*). Conformational and/or dynamic changes induced by the blue-light excitation have been assumed to be responsible for controlling the antirepressor activity of the AppA (*6*, *9*); however, whether these structural changes are actually induced by illumination remains unclear. Illuminating AppA induces a small but distinct red-shift of the FAD absorption in the UV−visible region, and the change was reversed in the dark (*6*, *9*). The molecular mechanisms behind the photocycle, however, are largely unknown. The photocycle is unique as compared with other photoreceptors, in which light absorption induces relatively large spectroscopic and structural changes of chromophores. The PAC protein in the green algae *Euglena gracilis* requires blue-light irradiation for its adenylate cyclase activity (*7*); however, photochemical properties of PAC have not been

[†] This work was supported by grants for the Frontier Research System and Special Postdoctoral Researchers Programs (to S.M. and K.H.) at RIKEN, and a Grant-in-Aid for Young Scientists (B) (15770101) (to K.H.) from MEXT of Japan.

* To whom correspondence should be addressed. Tel: +81(22)228 2046. Fax: +81(22)228 2045. E-mail: takaaki@postman.riken.go.jp.

[‡] S.M. and K.H. contributed equally to this work.

[1] Abbreviations: BLUF, sensor of blue-light using FAD; FAD, flavin adenine dinucleotide; FTIR, Fourier transform infrared; LOV, light, oxygen, or voltage.

10.1021/bi049836v CCC: $27.50
Published on Web 04/10/2004

characterized. Therefore, it is not clear whether the photocycle found in AppA is common to the sensor of blue-light using FAD (BLUF) domains.

A computer-aided DNA database search has indicated that proteins with the sequences homologous to the FAD-binding fold of AppA and PAC are distributed at least over 15 or more organisms. These proteins retain a novel structural and functional motif, suggesting that this FAD-binding fold is a new family of blue-light "perception domains" that function to control diverse biological processes in response to blue-light. Recently, this class of FAD-binding fold was proposed as a domain designated as BLUF (*8*).

An orf *slr1694* in the cyanobacterium *Synechocystis* sp. PCC 6803 encodes a 17 kDa protein with one BLUF domain (*8*). Slr1694 has been reported to retain noncovalently associated FAD and was suggested to be involved in phototaxis events in this cyanobacterium based on the gene disruption experiments (*10*). In the present study, we demonstrate that Slr1694 shows the same UV−visible spectral change upon illumination as that of AppA. This indicates that Slr1694 exhibits an AppA-like photocycle. The light-induced structural changes of the flavin chromophore and the apo-protein, which may be responsible for mediating the blue-light signaling, have been characterized by means of light-induced FTIR difference spectroscopy. This study is the first detailed spectroscopic characterization of a full-length BLUF protein.

MATERIALS AND METHODS

Construction of Expression Plasmid. The ORF Slr1694 of *Synechocystis* sp. PCC 6803 was overexpressed in *Escherichia coli* using a T7 RNA polymerase-based overexpression system with a self-cleavable intein/chitin tag (New England Biolabs). For this construction, forward and reverse primers 5′-TGCGGCCATATGAGTTTGTACCGTTTG-3′ and 5′-GGGAATTCTTAGAGGTCGAGGAAAAAG-3′ were used to amplify the *slr1694* coding sequence that contains *Nde*I and *Eco*RI sites (underlined), respectively. The amplified fragment was cloned into *Nde*I-*Eco*RI-cut pTYB12 (New England Biolabs) in order to generate a plasmid pTYSlr1694.

Protein Purification. The expression plasmid was transformed into *E. coli* strain BL21(DE3) (Novagen), and Slr1694 was overexpressed by induction with 1 mM isopropyl β-D-thiogalactopyranoside at 18 °C for 16 h in an M9 minimum medium. For uniform isotope labeling, the culture was grown using 18 mM $^{15}NH_4Cl$ (99.3% ^{15}N enrichment, Shoko Tsusho) for ^{15}N labeling or 11 mM glucose-U-^{13}C (98.3% ^{13}C enrichment, Shoko Tsusho) for ^{13}C labeling. Harvested cells suspended in a medium containing 0.5 M NaCl, 0.2 mM EDTA, and 20 mM Tris/HCl (pH 8.0) were ruptured with a chilled Bead-Beater (Biospec Products) for 2 min, and the soluble fraction was collected after centrifugation at 28 000*g* for 30 min. The Slr1694 protein was purified with a chitin affinity column using a protocol described by manufacture (New England Biolabs). The protein was dialyzed overnight at 4 °C against 0.3 M NH_4HCO_3 (pH 7.9), lyophilized, and then stored at −20 °C until use. The protein was dissolved in a H_2O (D_2O) medium containing 50 mM Tris/HCl (DCl) and 1 mM NaCl (pH (pD) 8.0) at a concentration of 0.3 mM protein and incubated for 1 h at 4 °C. Slr1694 showed no property change upon lyophilization.

Biochemical Analyses. The purity of the protein was estimated to be greater than 98% based on the densitometric intensity of Coomassie stained band of an SDS−PAGE gel on overloading conditions. The purified protein was fractionated in the dark on a Superose 6 PC 3.2/30 column (Amersham Biosciences) equilibrated with a medium containing 20 mM Tris/HCl (pH 8.0) and 100 mM NaCl. The apparent molecular mass of an eluted protein fraction was estimated by the use of standard proteins, including ferritin (450 kDa), albumin (68 kDa), chymotrypsinogen A (25 kDa), and cytochrome *c* (12.5 kDa).

Spectroscopic Measurements. For FTIR measurements, the sample solution (~6 μL) applied on a BaF_2 disk was gently dried by N_2 gas for several minutes. A droplet of 1 μL of 40% glycerol/H_2O (D_2O) (v/v) solution was placed outside of the IR beam on a disk for hydration (deuteration). The sample was subsequently sandwiched by the disks, spaced with a 0.5 mm thick Teflon spacer. The IR sample was incubated at 15 °C for 3 h in the dark in order to equilibrate the water present in the sample as described (*11*). For UV−visible absorption and fluorescence measurements, the protein sample solution was diluted with a H_2O (D_2O) medium containing 50 mM Tris/HCl (DCl) and 1 mM NaCl [pH (pD) 8.0] supplemented with various concentrations of glycerol when indicated. FTIR spectra were recorded using a Bruker IFS66v/s spectrophotometer with a MCT detector (EG&G Optoelectronics D316/6) at 15 °C and 4 cm^{-1} resolution by averaging 32 scans (20 s accumulation). A Ge band-pass filter (4000−800 cm^{-1}) (OCLI) was placed on both sides of the sample to improve the signal-to-noise ratio. The sample temperature was maintained using a homemade cryostat and temperature controller (Chino, KP1000) (*12*). A light minus dark spectrum was obtained by subtracting the single-beam dark spectrum from that following illumination for 10 s with continuous light (350−550 nm). Five to nine spectra were collected by repeating this cycle with a 1 h dark interval, upon which the sample fully relaxed to a dark state. No sample damage was detected during the measurements. A light-induced UV−visible absorption change was measured for FTIR sample, which was sandwiched between BaF_2 disks when indicated. UV−visible spectra were recorded on a SHIMAZU Multi Spec-1500 photodiode array spectrophotometer at 20 °C. Fluorescence emission spectra were recorded on a HITACHI F-4500 fluorescence spectrometer at 20 °C. Samples were illuminated with saturating white light for 5 s.

RESULTS

Slr1694 Protein. Figure 1 shows the elution profile of the purified Slr1694 on a size exclusion chromatography monitored at 280 and 450 nm for protein and flavin absorption, respectively. Almost all of the applied protein was eluted from the column as a single peak with a FAD bound form. Calibration of the column with the standard molecular marker proteins showed that Slr1694 was eluted at an apparent molecular mass of approximately 60 kDa (see inset figure). By considering the molecular mass of 17 kDa of Slr1694, the result indicates that Slr1694 exists in solution as a stable oligomeric form (trimer or tetramer) although the exact number of the subunit could not be determined. The result may suggest that Slr1694 functions as an oligomeric form in vivo.

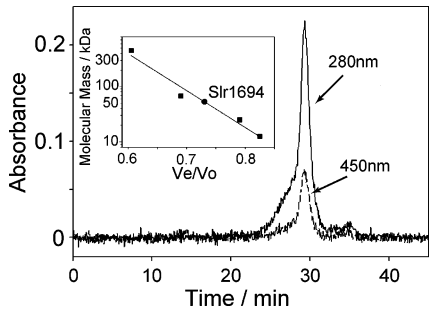

FIGURE 1: Elution profile of purified Slr1694 chromatographed in a Superose 6 PC 3.2/30 column and detected at 280 and 450 nm. Inset: A standard curve drawn according to peak elution volumes (V_e, elution volume; V_o, column volume) for the gel filtration standards (squares), including ferritin (450 kDa), albmine (68 kDa), chymotrypsinogen A (25 kDa), and cytochrome *c* (12.5 kDa). The position of Slr1694 is shown (circle).

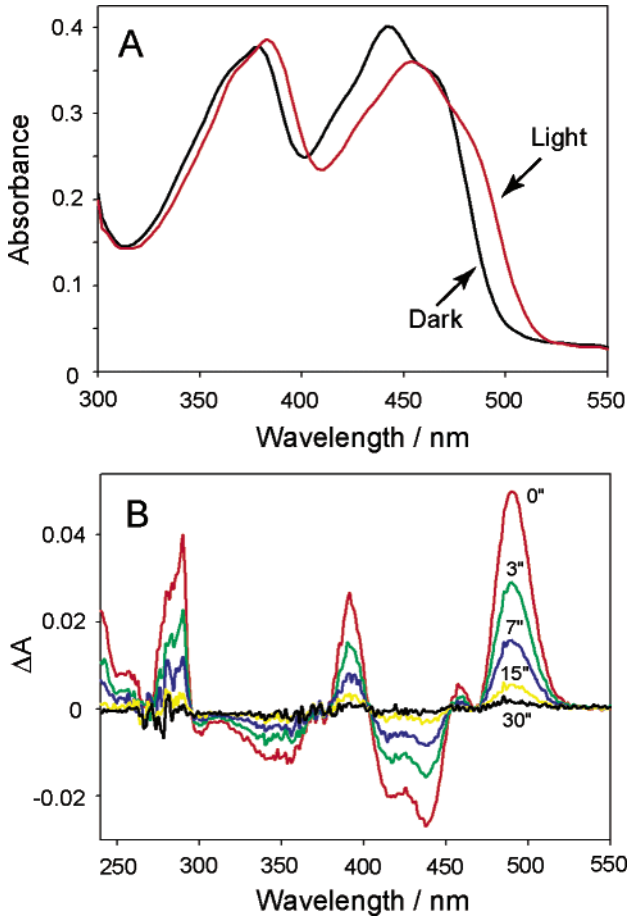

FIGURE 2: (A) UV−visible absorption spectra of dark-adapted (black line) and light-excited (red line) Slr1694. (B) Light minus dark difference spectra of Slr1694. Spectra were collected at 0, 3, 7, 15, and 30 s after illumination. See text for details.

Light-Induced Change in UV−Visible Spectra. Figure 2 shows the UV−visible absorption spectra of dark-adapted and light-excited Slr1694 (panel A) and the light minus dark difference (panel B) spectra in the photocycle of the purified Slr1694. A spectrum of dark-adapted Slr1694 exhibits two broad absorption peaks at 378 and 443 nm and shoulders at 363 and 471 nm (panel A, black line). These features are characteristics of oxidized flavin and very similar to those of AppA (*6*, *9*) with the exception of the minor differences at 340−370 nm. It is important to note that the spectrum was red-shifted by approximately 10 nm at the long wavelength end (panel A, red line) upon illumination, in which new peaks at 384 and 457 nm with shoulders at 367 and 483 nm were observed. Although the absorption spectra of Slr1694 were slightly different from those of AppA (*6*, *9*), the light minus dark difference spectrum in Slr1694 shown in panel B was surprisingly similar to that reported in AppA. This indicates that illumination induces the identical change in the FAD-binding site in both Slr1694 and AppA. The light-induced spectrum decayed to the dark spectrum with no change in spectral features. The photocycle could be repeated at least 10 times with no apparent sample damage.

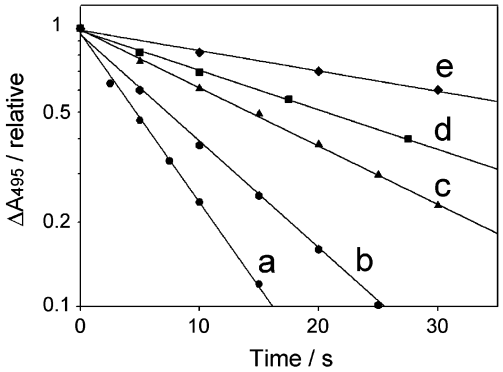

FIGURE 3: Decay kinetics of the light-induced UV−visible absorption changes (recorded at 495 nm) of Slr1694. Slr1694 was dissolved in a H_2O medium containing 50 mM Tris/HCl and 1 mM NaCl (pH 8.0) supplemented with no addition (a), 30% (v/v) glycerol (b), 50% (v/v) glycerol (c), and a D_2O medium containing 50 mM Tris/DCl and 1 mM NaCl (pD 8.0) (d). Alternatively, FTIR sample sandwiched between BaF_2 disks as described in the Materials and Methods was directly applied to UV−visible measurements (e).

Figure 3 shows the dark decay kinetics of the light-excited state in various conditions. The light-induced spectral change of Slr1694 decayed to the dark state monophasically, although the presence of a minor component with much slower decay time cannot be completely excluded. The results indicate that the light-excited state decays to the dark state with no intermediate state in accordance with no spectral change during the decay course as shown in Figure 2B. The half-life ($t_{1/2}$) for the light-excited state of Slr1694 (~5 s) is significantly shorter than that of AppA (~15 min) (*6*). The back reaction in the deuterated Slr1694 ($t_{1/2}$ of approximately 20 s) was four times slower than in the hydrated Slr1694, indicating that the decay (perhaps also formation) of the light-excited state involves H^+ transfer and/or rearrangement of hydrogen bondings, which limit the overall back reaction rate. Interestingly, a similar deuteration effect has been reported in the back reaction from the light-induced flavin−cysteinyl covalent adduct to the dark state in the LOV2 domain of phot1 (*13*, *14*). The dark decay of the light-excited state of the FTIR sample was much slower than that of the sample in solution, presumably due to lower water content in the FTIR sample. Again, similar decay trends have been reported in the phot1 LOV2 domain (*15*). The retardation of the dark decay was also observed when the protein solution included high concentration of glycerol. The back reaction rate in the presence of 30 and 50% (v/v) glycerol slowed to show $t_{1/2}$ of approximately 7 and 14 s, respectively. The observed effect of glycerol may be partially attributed to the decrease of water content, although the detailed

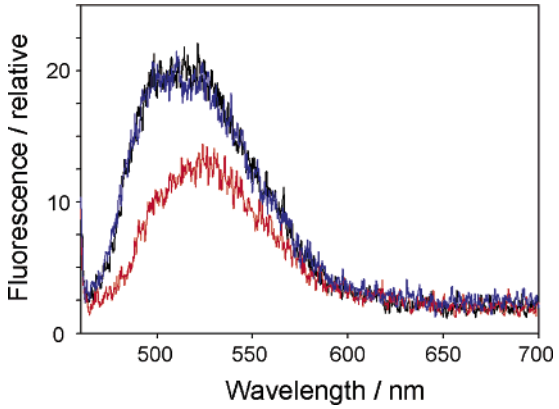

FIGURE 4: Fluorescence emission spectra (λ_{ex} = 450 nm) of Slr1694. Dark-adapted Slr1694 (black line) was illuminated with a continuous white light for 5 s, and then, the spectrum for the light-excited Slr1694 was acquired in the dark within 15 s (red line) and after incubation for 5 min (blue line).

mechanism is not clear at present. It is of note that the dark state spectrum and the light-induced spectral change in the FTIR and the glycerol-containing sample were identical to those of the Slr1694 in the buffer solution and completely decayed to the dark adapted state after prolonged dark incubation (data not shown).

As shown in Figure 4, the light illumination of Slr1694 induced marked quenching of the fluorescence from FAD. The maximum of the fluorescence spectrum of the light-excited Slr1694 was upshifted by approximately 10 nm in accordance with the upshift of the absorption spectrum by illumination as shown in Figure 2, and the dark state spectrum was restored after dark incubation. These properties are largely compatible with those reported for AppA (*9*) despite a relatively smaller quenching extent in Slr1694 than AppA. This difference is mainly ascribed to the much faster decay rate of the light-excited state in Slr1694 than AppA. The result indicates that the local environment of FAD is changed upon illumination. In this experiment, the sample solution included 50% (v/v) glycerol to retard the dark decay of the light-excited state during the fluorescence measurement, which took approximately 15 s, which corresponded with the half-decay time of the light-excited state in the presence of 50% (v/v) glycerol. These UV−visible absorption and fluorescence spectroscopic properties clearly demonstrate that Slr1694 exhibits the characteristic photocycle for the blue-light photoreceptor based on BLUF.

Light-Induced Change in FTIR Spectra. Light-induced structural changes in the FAD chromophore and the Slr1694 protein moiety during the photocycle have been evaluated by means of light-induced FTIR difference spectroscopy. Figure 5 shows the light minus dark FTIR difference spectra (1800−1000 cm^{-1}) (a−c) and absorption spectra of the dark state (d) for Slr1694. The negative and positive bands shown in the light-induced FTIR difference spectrum are assigned to those for the dark and light-excited states, respectively. Prominent bands appear at 1713−1510 cm^{-1}, while much weaker bands appear below 1510 cm^{-1}. The UV−visible spectrum for the dark-adapted FTIR sample was identical to that for the sample solution, and the identical spectral change was induced by illumination despite much slower course of dark decay of the light-excited state as shown in Figure 3. The course of dark decay for the IR bands was

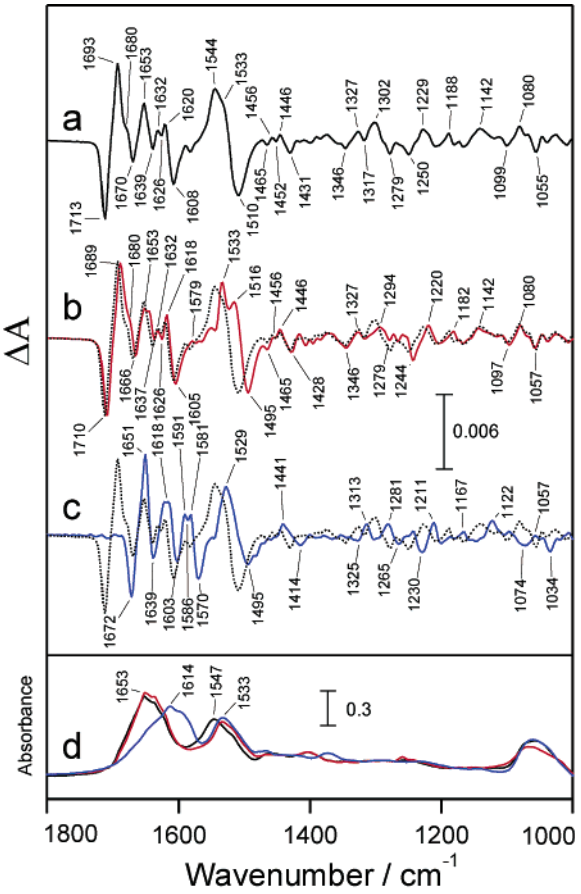

FIGURE 5: Effects of isotope labeling on light minus dark FTIR difference spectra (a−c) and IR absorption spectra (d) of hydrated Slr1694. Unlabeled (a and d, black lines; b and c, black-dotted lines), ^{15}N-labeled (b and d, red lines), and ^{13}C-labeled (c and d, blue lines) spectra.

similar to that of the light-induced UV−visible spectrum, and eventually, an identical FTIR spectrum was induced by illuminating the sample with higher water content, although the spectral quality was relatively low due to relatively large water band (data not shown). These indicate that the observed FTIR difference spectrum reflects structural changes of the flavin chromophore and/or apo-protein upon the formation of the light-excited state. The IR absorption spectrum of the dark-adapted Slr1694 (d, black line) exhibited the amide I and II peak at 1653 and 1547 cm^{-1}, which were mainly attributed to the C═O stretching mode (amide I) and the NH bending mode coupled to the CN stretching mode (amide II) of the polypeptide backbone. On the basis of the amide I peak position in the absorption spectrum, the secondary structure for Slr1694 is suggested to be comprised mainly of α-helixes.

Effects of ^{15}N/ ^{13}C Labeling on FTIR Difference Spectra. To characterize the light-induced IR bands, the effects of ^{15}N labeling (Figure 5b, red line) or ^{13}C labeling (Figure 5c, blue line) on the FTIR difference spectrum were studied. The prominent bands at 1713−1608 cm^{-1} in the unlabeled spectrum (dotted-black lines) downshifted only by 2−4 cm^{-1} upon ^{15}N labeling, whereas they downshifted by 31−42 cm^{-1} upon ^{13}C labeling, indicating that the bands are mainly ascribed to carbon-containing groups. The broad bands at 1544(+), 1533(shoulder), and 1510(−) cm^{-1} downshifted by 5−17 cm^{-1} to give the 1533(+)/1516(+)/1495(−) cm^{-1}

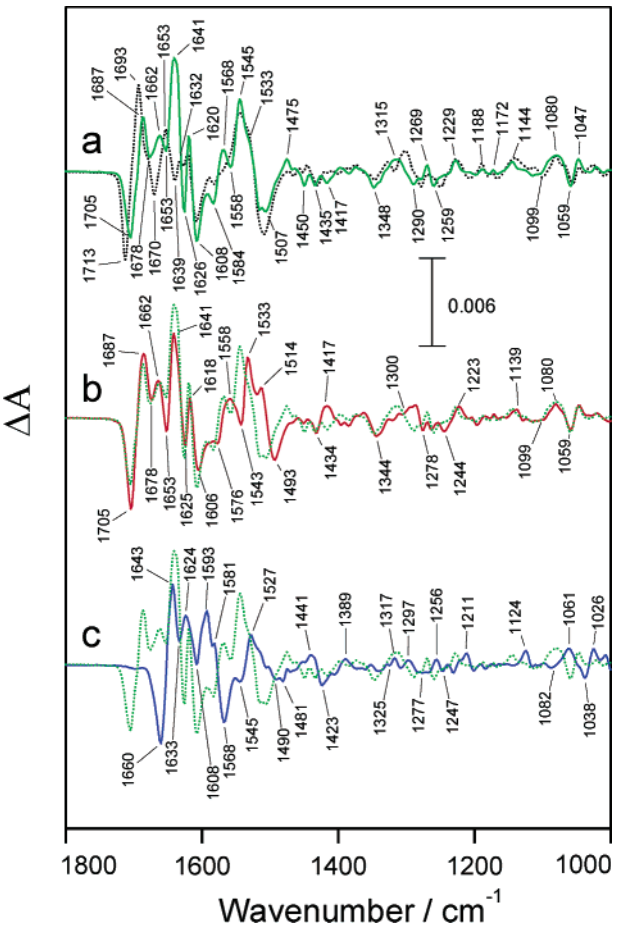

FIGURE 6: Effects of isotope labeling on light minus dark FTIR difference spectra of deuterated Slr1694. Unlabeled (a, green line; b and c, green-dotted lines), ^{15}N-labeled (b, red line), and ^{13}C-labeled (c, blue line) spectra. The spectrum of hydrated/unlabeled Slr1694 is also presented (a, black-dotted line).

bands upon ^{15}N labeling and the 1529(+)/1495(−) cm^{-1} bands upon ^{13}C labeling, indicating the contribution of groups containing both nitrogen and carbon atoms. Below 1460 cm^{-1}, almost all bands downshifted in the ^{13}C spectrum, but the ^{15}N spectrum was similar to the unlabeled spectrum with the exception of the 1325−1220 cm^{-1} region. Therefore, the bands below 1460 cm^{-1} are assigned to the groups containing carbon but not nitrogen atom, while the bands at 1325−1220 cm^{-1} were assigned to groups containing both nitrogen and carbon atoms. As shown in Figure 5d, the amide I absorption band at 1653 cm^{-1} consistently downshifted by 39 cm^{-1} upon ^{13}C labeling (blue line), and the amide II band at 1547 cm^{-1} downshifted by 14 cm^{-1} upon ^{13}C or ^{15}N labeling (red line).

Effects of Deuteration on FTIR Difference Spectra. Figure 6 shows the effects of deuteration on the light minus dark FTIR difference spectra, in which the lyophilized protein was dissolved in the D_2O buffer and incubated for 1 h at 4 °C. The spectrum of Slr1694 was largely altered upon deuteration (a, green line), indicating that groups influenced by illumination include exchangeable hydrogen present mostly in hydrophilic environments. The same deuteration effects were observed after 1 week of incubation of the protein in the D_2O buffer at 4 °C (data not shown). The 1713(−)/1693(+) cm^{-1} bands downshifted by ∼7 cm^{-1} to 1705(−) and 1687(+) cm^{-1}, and the 1670(−)/1653(+) cm^{-1} bands downshifted to yield prominent bands at 1641(+), 1626(−), and 1620(+) cm^{-1}. Furthermore, the deuterated spectrum shows distinct bands at 1584(−), 1568(+), and 1558(−) cm^{-1}, which may be harbored in the hydrated spectrum but did not appear as distinct bands due to the overlap of other bands and then disclosed by the downshifts of the overlapped bands by deuteration. The NH bending of the amide II vibrations is thought to be responsible for the modes affected by deuteration, as NH in-plane bending vibration of an isoalloxazine ring does not appear in this region (*16*). Deuteration also affected the spectrum at 1480−1200 cm^{-1}; several bands were newly appeared at 1475−1348 cm^{-1}, and the bands at 1302−1250 cm^{-1} upshifted by 9−13 cm^{-1}. The slight reduction in the 1510(−) cm^{-1} band intensity was probably due to the shift of the overlapped amide II bands. In contrast, the bands at 1544(+), 1533(shoulder), and 1200−1050 cm^{-1} were scarcely affected by deuteration.

Interestingly, the deuterate-effected bands at 1705−1606 cm^{-1} (b, green-dotted line) were not effected by ^{15}N labeling (b, red line). This observation is in contrast to the small but distinct downshift of the corresponding bands by ^{15}N labeling in the hydrated spectrum (Figure 5b, red line), indicating that the modes of groups containing no nitrogen are predominantly responsible for these bands. In the hydrated spectrum, these modes are coupled with the modes of groups containing both nitrogen and exchangeable hydrogen. The bands downshifted in good agreement with the theoretical value for the C═O stretching mode upon ^{13}C labeling in both the hydrated (Figure 5c, blue line) and the deuterated (Figure 6c, blue line) spectra. Therefore, it is rational to assume that C═O stretching vibrations are coupled with the modes, such as an NH bending in the hydrated spectrum. The deuterate-effected bands at 1475−1348 cm^{-1} were affected in complex manners by ^{15}N or ^{13}C labeling, probably due to overlapping of CN stretching mode, which was downshifted from the amide II vibrations (∼1580 cm^{-1}) by decoupling upon deuteration. In contrast, the bands at 1475−1348 cm^{-1} in the hydrated spectrum were little affected by ^{15}N labeling (Figure 5b, red line) and downshifted upon ^{13}C labeling (Figure 5c, blue line). These bands are ascribed to the vibrations from groups containing carbon and/or exchangeable hydrogen but lacking nitrogen, namely, CC stretching and/or CH_3 asymmetric bending. The deuterate-upshifted bands at 1315(+), 1290(−), and 1259(−) cm^{-1} [1302(+), 1279(−), and 1250(−) cm^{-1} in the hydrated spectrum] downshifted by 12−20 and 5−8 cm^{-1} upon ^{15}N (Figure 6b, red line) and ^{13}C (Figure 6c, blue line) labeling. Therefore, groups containing nitrogen, carbon, and exchangeable hydrogen are responsible for these bands, which may be mainly attributed to the CC and CN stretching vibrations coupled with the NH bending mode.

The 1544(+)/1533(shoulder)/1510(−) cm^{-1} bands in the hydrated spectrum (Figures 5a and 6a, black-dotted lines) were only slightly affected by deuteration and largely downshifted upon both ^{15}N and ^{13}C labeling. Therefore, the groups containing both carbon and nitrogen, but not exchangeable hydrogen, are responsible for these bands, indicating the contribution of the CN stretch vibration that does not couple with an NH bending mode. The 1584(−)/1568(+)/1558(−) cm^{-1} bands (Figure 6a, green line) appeared by deuteration are also attributable to the CN stretch vibration, which does not couple with an NH bending mode as the bands are largely downshifted upon ^{15}N and ^{13}C

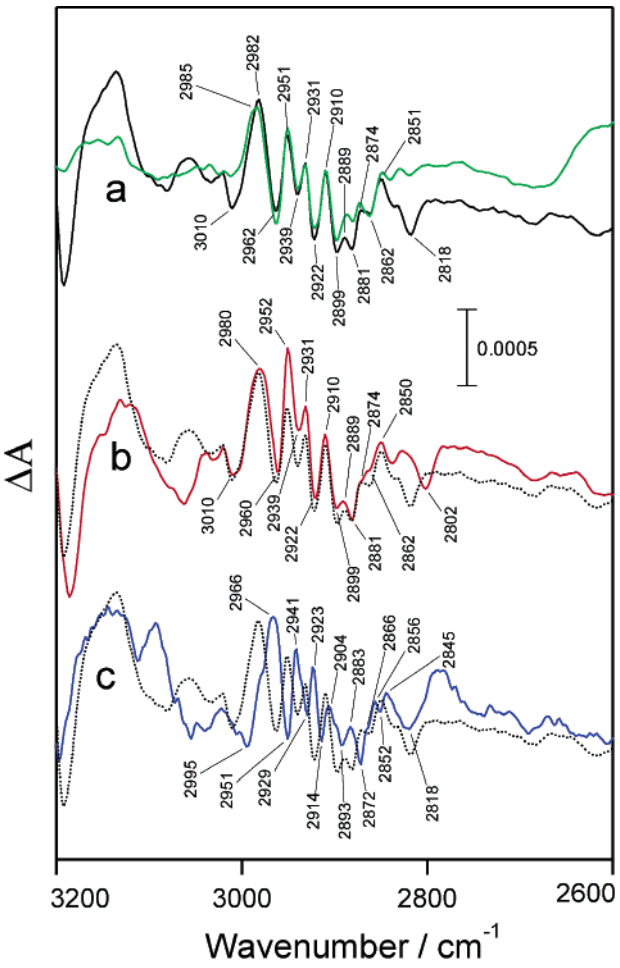

FIGURE 7: High-frequency region (3200−2600 cm^{-1}) of the light minus dark FTIR spectra of Slr1694. Unlabeled spectra of hydrated (a, black line; b and c, black-dotted lines) and deuterated (a, green line) Slr1694 and ^{15}N-labeled (b, red line) and ^{13}C-labeled (c, blue line) spectra of hydrated Slr1694.

labeling. The deuterate insensitive bands at 1200−1000 cm^{-1} were not affected by ^{15}N labeling (Figure 6b, red line) but downshifted by ~20 cm^{-1} upon ^{13}C labeling (Figure 6c, blue line), indicating that the groups containing carbon but neither nitrogen nor exchangeable hydrogen are responsible for the bands. Possible candidates are the bending vibrations of CH and CH_2, the stretching vibrations of CC and C−CH_3, and CH_3 rocking.

High-Frequency FTIR Difference Spectra. Figure 7 shows the effects of deuteration (a), ^{15}N labeling (b), or ^{13}C labeling (c) on the higher frequency spectrum, in which the CH stretching modes of the CH (3200−3000 cm^{-1}), and CH_2 and CH_3 (3000−2800 cm^{-1}) groups are expected to appear (*17*). The bands in the hydrated spectrum (a, black line; b and c, black-dotted lines) were observed to downshift upon ^{13}C labeling (c, blue line) by 5−16 cm^{-1} but were little affected upon deuteration (a, green line) or ^{15}N labeling (b, red line). Therefore, the bands are ascribed to the groups containing carbon but neither nitrogen nor exchangeable hydrogen. The observed shifts by ^{13}C labeling coincide with the shifts expected for CH stretching of CH_2 and CH_3 groups. Generally, a CH_3 group shows two stronger asymmetric and one weaker symmetric CH_3 stretching bands at 3000−2900 and 2900−2800 cm^{-1}, respectively (*17*). Figure 7a shows the presence of stronger bands at 3010−2910 cm^{-1} and weaker bands at 2899−2851 cm^{-1}. If the three pairs of bands at 2899(−)/2889(+), 2881(−)/2874(+), and 2862(−)/2851(+) cm^{-1} are ascribed to the symmetric CH_3 modes, at least three CH_3 groups are attributable to the bands. The 2818(−) cm^{-1} band disappeared upon deuteration (a, green line) and largely downshifted upon ^{15}N labeling (b, red line) but was not affected by ^{13}C labeling (c, blue line), indicating a contribution of group containing both nitrogen and exchangeable hydrogen but not carbon, namely, NH. The absence of a sharp band from the CH group at 3200−3000 cm^{-1} indicates that this group does not contribute to the spectrum, indicating no light-induced structural change of Slr1694 in the moiety including CH group.

Possible modes for the main bands found in the FTIR difference spectrum at 1800−1000 cm^{-1} are summarized in the Table 1, in which the band positions in the hydrated spectrum, and band shifts upon ^{15}N ($\Delta^{15}N$) or ^{13}C ($\Delta^{13}C$) labeling in the hydrated and deuterated spectra are also presented, in addition to possible assignments of the bands (see Discussion).

DISCUSSION

Slr1694. The present results demonstrated that illumination of Slr1694 of *Synechocystis* sp. PCC6803 exhibits a photocycle with the same changes in the UV−visible absorption and FAD fluorescence emission spectra as reported for AppA (*6*, *9*). Taking this into account together with the influence of the negative phototaxis in *slr1694* disruptant (*10*) and the presence of the BLUF domain (*8*), we conclude that Slr1694 is a novel BLUF protein and may be involved in some blue-light perception event in *Synechocystis*, although the exact physiological function of Slr1694 in vivo has not been completely defined at present. The present results showed that the light-induced spectral change in the UV−visible absorption is the common characteristic feature of the BLUF proteins. Some cyanobacterial species have exhibited negative and positive phototactic movement in response to blue light (*18*, *19*), but the photoreceptor for the phototactic responses to blue light has not been defined except for the indication that cyanobacterial phytochrome Cph2 is involved in inhibiting the positive phototactic movement toward blue light (*18*). Therefore, it may be possible to assume that Slr1694 is involved in the phototaxis in response to blue light as a photoreceptor. In general, the light perception process is triggered by light-induced redox reaction and/or structural rearrangements of chromophore of the photoreceptor, and these changes are translated into structural changes in protein moiety, thereby inducing a signaling state of the photoreceptor. In photoreceptors based on flavin, the structural change of flavin (FMN) is accompanied by the formation of a covalent flavin−cysteinyl adduct in the LOV domain of phototropins (*15*, *20*−*24*). Alternatively, flavin (FAD) functions as a redox center, which is photooxidized to induce inter- and/or intraprotein electron transfer in cryptochrome (*2*, *25*). Although a relatively small photoinduced absorption shift suggests neither redox change nor gross structural rearrangements of FAD in BLUF, little is known about what change is actually induced in flavin upon illumination and whether this change in chromophore is accompanied by a structural change of the protein moiety. Slr1694 is thought to be an ideal system to further explore these questions, since it is a small protein consisting of a

Table 1: FTIR Bands Positions in Hydrated Slr1694, Shifts upon $^{15}N/^{13}C$ Labeling and Deuteration, and Predominant Assignments of the Bands

bands positions and shifts (cm^{-1})				
hydrated bands	$\Delta^{15}N$	$\Delta^{13}C$	possible candidates[a]	predominant assignments[a]
1713(−)[b] [−8][c]	−3[d] {0}[e]	−41[f] {−45}[g]	ν(CO)	ν_{FAD} (C4═O)
1693(+) [−6]	−4 {0}	−42 {−44}	ν(CO)	ν_{FAD} (C4═O)
1670(−) [−17]	−4 {0}	−31 {−45}	ν(CO), δ(NH)	ν_{FAD} (C2═O)
1653(+) [−12]	0 {0}	−35 {−48}	ν(CO), δ(NH)	ν_{FAD} (C2═O)
1639(−) [ND]	−2 {ND}	−36 {ND}	ν(CO), ν(CC)	amide I
1632(+) [ND]	0 {ND}	−41 {ND}	ν(CO), ν(CC)	amide I
1626(−) [0]	0 {−1}	−40 {−45}	ν(CO), ν(CC)	amide I
1620(+) [0]	−2 {−2}	−39 {−39}	ν(CO), ν(CC)	amide I
1608(−) [0]	−3 {−2}	−38 {−40}	ν(CO), ν(CC)	amide I
1544(+) [0]	−11 {−11}	−15 {−17}	ν(CN)	ν_{FAD} (C4aN5)/ν_{FAD}(N1C10a)
1533(+) [0]	−17 {−19}	−25? {−17}	ν(CN)	ν_{FAD} (C4aN5)/ν_{FAD}(N1C10a)
1510(−) [−3]	−5 {−14}	−5 {−17}	ν(CN), δ(NH)	ν_{FAD} (C4aN5)/ν_{FAD}(N1C10a) and amide II
1446* (+) [0]	0 {0}	−5 {−5}	δab(CH_3), ν(CC)	side chain or $\delta ab_{FAD}(CH_3)$
1431* (−) [0]	−3 {−3}	−17 {−8}	δab(CH_3), ν(CC)	side chain or $\delta ab_{FAD}(CH_3)$
1346* (−) [+2]	0 {−4}	−21 {−23}	ν(CN), ν(CC), δ(NH), δsb(CH_3)	ν_{FAD} (N3C4)
1302* (+) [+13]	−8 {−15}	−21 {−18}	ν(CN), ν(CC), δ(NH), δsb(CH_3)	ν_{FAD} (N3C4)
1279* (−) [+11]	0 {−12}	−14 {−13}	ν(CN), ν(CC), δ(NH), δsb(CH_3)	ν_{FAD} (N3C4)
1250* (−) [+9]	−6 {−15?}	−20 {−12?}	δ(NH), ν(CC), ν(CN), δ(CH)	ν_{FAD} (N3C4)
1142* (+) [+2]	0 {−5}	−20 {−20}	$\rho(CH_3)$, ν(CC), δ(CH)	side chain or $\rho_{FAD}(CH_3)$
1099* (−) [0]	−2 {0}	−25 {−17}	$\rho(CH_3)$, ν(CC), δ(CH)	side chain or $\rho_{FAD}(CH_3)$
1080* (+) [0]	0 {0}	−23 {−19}	$\rho(CH_3)$, ν(CC), δ(CH)	side chain or $\rho_{FAD}(CH_3)$
1055* (−) [+4]	0 {0}	−16 {−21}	$\rho(CH_3)$, ν(CC), δ(CH)	side chain or $\rho_{FAD}(CH_3)$

[a] Abbrevations for assignments: ν, stretching; δ, bending; δab, asymmetry bending; δsb, symmetry bending; ρ, rocking. [b] Positive and negative signs correspond to positive and negative bands. [c] Shifts upon deuteration. [d] Shifts of hydrated bands upon ^{15}N labeling. [e] Shifts of deuterated bands upon ^{15}N labeling. [f] Shifts of hydrated bands upon ^{13}C labeling. [g] Shifts of deuterated bands upon ^{13}Clabeling. ND, not determined due to overlapping of C2═O stretch vibration. *Bands with small intensities.

single BLUF domain, and it can be expressed as a functional full-length protein and purified with full photocycling capability.

Light-Induced Structural Changes of Slr1694. The light-induced FTIR difference spectrum showed prominent bands above 1500 cm^{-1}, while much weaker bands were detected at 1500−1000 cm^{-1}, the region in which strong IR bands for the skeletal vibrations of a flavin isoalloxazine ring are expected to appear (*26*, *27*). In fact, the light-induced FTIR difference spectrum of the LOV2 domain shows many intense bands in this frequency region (*15*, *28*). The absence of these strong bands therefore indicates that gross structural rearrangements of the isoalloxazine ring do not occur upon illumination in Slr1694. The bands observed in the FTIR spectrum have been assigned to the amide modes of protein moiety as well as the modes for a FAD isoalloxazine ring according to their position and the effects of the isotopes as enunciated in the second half of the discussion part, and the predominant assignments were included in Table 1.

The C4═O and C2═O stretch vibrations of the isoalloxazine ring (see Figure 8) in the dark state Slr1694 are responsible for the 1713(−) and 1670(−) cm^{-1} bands, which downshift by 20 and 17 cm^{-1} upon illumination to yield 1693(+) and 1653(+) cm^{-1} bands, respectively. The bands' positions in the dark state are between those of the free and strongly H-bonded state in solution (*26*, *29*, *30*). Hydrogen bonding is known to downshift the C═O stretching vibrational frequency (*29*, *30*). Therefore, we indicate that the C4═O and C2═O are moderately hydrogen bonded in the dark state and strongly hydrogen bonded to the peptide backbone and/or amino acid side groups in the light-excited state. Interestingly, the C4═O forms a strong hydrogen bond with the NH in the peptide backbone to show a band at 1693 cm^{-1} in substrate-bound short chain acyl-CoA dehydrogenase

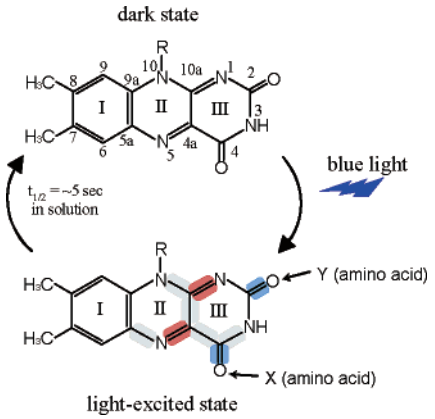

FIGURE 8: Light-induced changes in force constants in FAD isoalloxazine ring defined by FTIR during the photocycle of Slr1694. Bonds that are weakened or strengthened are highlighted in blue or red, respectively. Bonds with small strength changes are highlighted in gray. X and Y represent residues that are strongly hydrogen bonded to C2═O and C4═O upon illumination, respectively. See text for details.

(*30*). It is of note in this context that the intensity of the C4═O band at 1713(−) cm^{-1} was found to be much stronger than that of the C2═O band at 1670(−) cm^{-1}. The two bands have been reported to be of similar intensity in flavin, which has no hydrogen bonding at C2═O and C4═O (*16*, *27*). The observed intensity difference may reflect the difference of the hydrogen bonding states between the C2═O and the C4═O groups. Table 1 indicates that the coupled N1C10a and C4aN5 stretch vibrations are responsible for the 1544(+) and 1533(+ shoulder) cm^{-1} bands in the light-excited state and the 1510(−) cm^{-1} band in the dark state. The dark bands appeared at considerably low frequencies and were upshifted relative to those of a flavin in solution upon illumination, indicating that N1C10a and/or C4aN5 bondings are relatively

weak in the dark state and strengthened in the light-excited state. As both modes are tightly coupled, it is difficult to distinguish whether the changes in the force constants are attributed to the combination of N1C10a and C4aN5 or one of the individual modes. Besides the prominent bands, the 1302(+)/1279(−)/1250(−) cm^{-1} bands are primarily ascribed to the N3C4/C4C4a/C4aC10a stretch modes of the isoalloxazine ring III, and the 1584(−)/1568(+)/1558(−) cm^{-1} bands, which appeared in the deuterated spectrum (see Figure 6a, green line), are attributed to the N5C5a and N10C10a modes, although the light-induced changes may be small. The details for the change in force constant of the respective bond cannot be defined due to low band intensities and/or mode couplings in these bands. The CH stretching frequency for CH_3 may contribute to the bands at 1480−1350 and 1200−1000 cm^{-1} as supported by the high-frequency spectra shown in Figure 7 and might be attributed to the CH_3(C7) and CH_3(C8). However, no light-induced structural change at C9H and C6H depicted by the absence of the CH stretching mode in the high-frequency spectrum indicates little structural rearrangements in the isoalloxazine ring I upon illumination. Therefore, it is feasible to assign these to the side chains of amino acids.

Figure 8 illustrates the light-induced changes in the isoalloxazine ring of FAD during the photocycle of Slr1694 deduced from the present study. The FTIR results demonstrate that light excitation results in the change in the force constants of the FAD isoalloxazine ring III (primarily) and ring II but small changes in the ring I. Illumination leads to the formation of strong hydrogen bonding interactions at O(═C2) and O(═C4), although their counterparts cannot be identified at present. An increased H-bonding interaction at N5 was proposed to cause the light-induced red-shift of the absorption spectrum in AppA (*9*). Contrary to this proposal, the strengthen force constants at C4aN5/N1C10a show the decrease of the putative interaction upon illumination. Alternatively, the deprotonation of the isoalloxazine ring has been thought to be responsible for the light-induced spectral changes (*31*). A deprotonated isoalloxazine ring has no exchangeable hydrogen; therefore, the bands for the light-excited state (positive bands in the FTIR spectrum) will be insensitive to deuteration. This was clearly not the case as shown in Figure 6a, which showed marked deuteration effects on the bands both for light-excited and the dark states. As shown in Figure 3, the decay rate of the light-excited form in D_2O is approximately four times slower than in H_2O as measured by UV−visible absorption change of chromophore, indicating that a rate limiting proton transfer reaction is involved in the decay process. No change in the protonation state of the FAD isoalloxazine ring upon illumination, therefore, suggests that the rate limiting proton transfer reaction and/or alteration of hydrogen bondings occur in the protein moiety. These changes may be responsible for the observed light-induced changes of the amide I mode and cause the change in hydrogen bonding interaction between the FAD isoalloxazine ring and the protein. The changes of the amide I mode appeared predominantly at 1639−1608 cm^{-1}, indicating that structural changes in the protein moiety including β-sheets and/or turns are mainly induced (*17*), despite the high α-helix content of Slr1694. This view is consistent with the finding that almost the light-induced bands were influenced by deuteration (Figure 6), indicating that the light-induced changes occur in the region in hydrophilic environments. The analysis using size exclusion chromatography revealed that Slr1694 exists in a stable oligomeric form in solution as shown in Figure 1. Therefore, the structural changes of the protein moiety may alter the interactions between the subunit monomers and induce quaternary structural change of the oligomer thereby inducing the signaling state.

A NMR study on AppA indicated the presence of $\pi-\pi$ stacking interactions in the FAD isoalloxazine ring and that the interaction was affected by illumination (*9*). Both the stacking interaction and the photocycle were impaired by a site-directed change of Tyr21, which is conserved in all putative BLUF domains to the authors' knowledge. Therefore, the changes in $\pi-\pi$ stacking interactions between the phenol ring of the tyrosine residue and the isoalloxazine ring (mainly ring III and secondarily ring II) may be partly responsible for the observed light-induced changes in the force constants in Slr1694. In short chain acyl-CoA dehydrogenase, a FAD adenine ring parallels the isoalloxazine ring III in close vicinity (*32*). Therefore, we cannot completely exclude the possibility that the adenine ring is partly attributable to the $\pi-\pi$ stacking interactions and/or H-bonding interactions at O(═C4) and O(═C2).

Recently, a light-induced FTIR spectrum of C-terminal truncated AppA has been reported (*31*), but the spectrum was significantly different from the present Slr1694 spectrum. The AppA spectrum showed the strong bands at 1710(−) and 1698(+) cm^{-1}, which were assigned to the C4═O stretching in this study, but the other bands had a much smaller intensity. Notably, there was no prominent band at 1680−1300 cm^{-1} in the AppA. Although at present the origin of these differences is unclear, it is important to emphasize that the FTIR difference spectra were obtained for the full-length protein in this study, whereas the spectra for the BLUF domain of C-terminal truncated AppA were taken (*31*). The BLUF domain of AppA shows light-induced changes in the UV−visible spectrum, which is nearly identical to those of Slr1694 (*6*, *9*). Therefore, a straightforward interpretation of the observations is that the decrease in the C4═O bond strength is sufficient to actualize the spectral red-shift, and the light-induced absorption change of FAD is not necessarily accompanied by changes in the C2═O mode, the N1C10a and/or C4aN5 stretching vibrational modes, and the amide I mode, which are thought to be responsible for the photoreceptor signal translating function of Slr1694. Ab initio molecular orbital calculation of isolumazine (a model of flavin) indicated that H-bonding to O(═C4), O(═C2), and N3H causes the red-shift (*33*). Therefore, we may conclude that the bands photoinduced in Slr1694 but not in AppA reflect propagating structural changes important for the signal translating function of BLUF.

An unanswered question is how these changes are induced by the light absorption of the FAD chromophore. Preferential electron charge distribution of the lowest unoccupied molecular orbital at N5 of an isoalloxazine ring in photoexcited triplet state of FAD (*34*) may facilitate the $\pi-\pi$ stacking interactions in the FAD isoalloxazine ring. Alternatively, a short-lived precursor intermediate state may also be formed as a direct product of the photoexcited FAD triplet state, which subsequently becomes the spectroscopically defined light-excited state.

Predominant Assignments of FTIR Bands. Numerous Raman and IR spectra have been reported for various flavin compounds (*16*, *26*, *27*, *30*, *35*−*38*) and flavoproteins (*15*, *24*, *28*, *31*, *39*−*42*), and the bands have been assigned by normal coordinate analysis using lumiflavin as a model of flavin in combination with specific isotope labeling techniques (*16*, *26*, *29*, *43*). As shown in Table 1, the bands at 1713−1608 cm^{-1} are mainly assigned to the C═O stretch vibration with minimal contributions from NH bending. The C4═O and C2═O stretch bands for an isoalloxazine ring appear at 1723−1687 and 1694−1647 cm^{-1} (*16*, *26*, *30*). Upon deuteration, the C4═O and C2═O stretch bands downshift by 1−13 and 12−30 cm^{-1} respectively, depending on the hydrogen bonding states of the C═O groups (*26*, *29*, *44*, *45*). On the basis of the strong agreement of the bands positions and the band-shifts upon deuteration, the negative bands at 1713 and 1670 cm^{-1} were reasonably assigned to the C4═O and C2═O stretches of the isoalloxazine ring for the dark state Slr1694. The derivative-shaped band pairs at 1713(−)/1693(+) cm^{-1} and 1670(−)/1653(+) cm^{-1} have features typical of those arising from band-shifts. Therefore, the positive bands at 1713 and 1670 cm^{-1} were assigned to the C4═O and C2═O stretch for the light-excited state of Slr1694, respectively. An isoalloxazine ring has no C═O group other than C2═O and C4═O; therefore, the C═O bands at 1639(−), 1632(+), 1626(−), 1620(+), and 1608(−) cm^{-1} can be assigned to the modes from the protein moiety. The C═O stretch vibrations of the protonated carboxylate side group appear at much higher frequencies (1750−1700 cm^{-1}). Asn and Gln residues are potentially involved in the C═O stretch vibrations in this region; however, the absence of ^{15}N-effected CN stretching bands for these residues at 1420−1400 cm^{-1} (Figure 5) indicates little light-induced formational change in these two residues. Therefore, these bands were assigned to the amide I vibrations. Accordingly, the amide I modes were responsible for the deuterated 1678(−)/1662(+) cm^{-1} bands (Figure 6a, green line), which are obscured by the C2═O stretch bands in the hydrated spectrum (Figure 6a, black-dotted line).

The prominent 1544(+)/1533(+shoulder)/1510(−) cm^{-1} bands were mainly assigned to the CN stretch vibration, which does not couple with the NH bending mode. Coupled C4aN5/N1C10a stretch vibrations from the isoalloxazine ring (*16*) may be responsible for these bands, although the contributions from amino acid side chains and/or adenine modes cannot be excluded completely. The C4aN5/N1C10a modes give a strong/broad band at 1552 cm^{-1} and a weak band at 1513 cm^{-1} in a lumiflavin solution (*26*). Consistently, the observed 1544(+)/1510(−) cm^{-1} bands showed strong IR intensity comparable to the C═O stretching vibrations at 1713 and 1670 cm^{-1}, and the 1533(+) cm^{-1} band was seen only as a broad shoulder. The negative counterpart of the 1533(+) cm^{-1} was not resolved well probably due to low intensity. Furthermore, the ^{15}N isotopic downshift of the bands (5−17 cm^{-1}) was compatible with that reported in ^{15}N-labeled lumiflavin (8−13 cm^{-1}) (*26*).

The CC and CN stretch coupled with NH bending is thought to be responsible for the bands at 1302−1250 cm^{-1} as shown in Table 1. The coupled CC and CN stretch vibrations for an isoalloxazine ring appear at 1350−1250 cm^{-1} and are upshifted upon deuteration due to the consequence of decoupling with N3H bending (*16*). Interestingly, the upshift has been reported to be ∼10 cm^{-1} for ring III but much smaller for ring I and ring II (*16*). The upshift of 9−13 cm^{-1} upon deuteration indicates that the bands at 1350−1250 cm^{-1} are mainly ascribed to the N3C4/C4C4a/C4aC10a modes of isoalloxazine ring III. The CN stretching bands, which appeared distinctly in the deuterated spectrum at 1584(−), 1568(+), and 1558(−) cm^{-1} (see Figure 6a), are attributable to the N5C5a and N10C10a modes of the isoalloxazine ring based on their positions (*16*).

CONCLUSIONS

The present results demonstrated that *Synechocystis* sp. PCC6803 Slr1694 shows almost identical light-induced changes in the UV−visible absorption spectrum with AppA but much faster back reaction rate from the light-excited state to the dark state, indicating that Slr1694 is a blue-light receptor based on BLUF. Light-induced FTIR difference spectroscopy in combination with stable isotope labeling indicated the relatively small FAD structural rearrangements and prominent structural changes in the protein moiety including proton transfer and/or rearrangement of hydrogen bonding interactions upon illumination. Recent NMR structural analysis of the phot1 LOV2 domain revealed light-induced gross structural rearrangements (*46*), which were not detected by crystallographic analysis (*21*, *22*) but were detected in FTIR studies (*15*, *28*). The present FTIR results provide crucial information for the understanding of the blue-light perception mechanism of the BLUF photoreceptor.

ACKNOWLEDGMENT

We thank Prof. Hellingwerf for a preprint and Dr. Mizusawa for genomic DNA of *Synechocystis*.

REFERENCES

1. Briggs, W. R., and Huala, E. (1999) Bule-light photoreceptors in higher plants, *Annu. Rev. Cell Dev. Biol. 15*, 33−62.
2. Lin, C. (2000) Plant blue-light receptors, *Trends Plant Sci. 5*, 337−342.
3. Sancar, A. (2003) Structure and function of DNA photolyase and cryptochrome blue-light photoreceptors, *Chem. Rev. 103*, 2203−2237.
4. Crosson, S., Rajagopal, S., and Moffat, K. (2003) The LOV domain family: photoresponsive signaling modules coupled to diverse output domains, *Biochemistry 42*, 2−10.
5. Cashmore, A. R. (2003) Cryptochromes: Enabling plants and animals to determine circadian time, *Cell 114*, 537−543.
6. Masuda, S., and Bauer, C. E. (2002) AppA is a blue light photoreceptor that antirepresses photosynthesis gene expression in *Rhodobacter sphaeroides*, *Cell 110*, 613−623.
7. Iseki, M., Matsunaga, S., Murakami, A., Ohno, K., Shiga, K., Yoshida, K., Sugai, M., Takahashi, T., Hori, T., and Watanabe, M. (2002) A blue-light-activated adenylyl cyclase mediates photoavoidance in *Euglena gracilis*, *Nature 415*, 1047−1051.
8. Gomelsky, M., and Klug, G. (2002) BLUF: a novel FAD-binding domain involved in sensory transduction in microorganisms, *Trends Biol. Sci. 27*, 497−500.
9. Kraft, B. J., Masuda, S., Kikuchi, J., Dragnea, V., Tollin, G., Zaleski, J. M., and Bauer, C. E. (2003) Spectroscopic and mutational analysis of the blue-light photoreceptor AppA: A novel photocycle involving flavin stacking with an aromatic amino acid, *Biochemistry 42*, 6726−6734.
10. Okajima, K., Yoshihara, S., Geng, X., Katayama, M., and Ikeuchi, M. (2003) Structural and functional analysis of a novel flavoprotein in Cyanobacteria, *Plant Cell Physiol. 44* (Suppl.), 162.
11. Noguchi, T., and Sugiura, M. (2002) Flash-induced FTIR difference spectra of the water oxidizing complex in moderately hydrated photosystem II core films: effects of hydration extent on S-state transition, *Biochemistry 41*, 2322−2330.

12. Kimura, Y., Mizusawa, N., Ishii, A., Yamanari, T., and Ono, T. (2003) Changes of low-frequency vibrational modes induced by universal ^{15}N- and ^{13}C-isotope labeling in S_2/S_1 FTIR difference spectrum of oxygen evolving complex. *Biochemistry 42*, 13170−13177.
13. Swartz, T. E., Corchnoy, S. B., Christie, J. M., Lewis, J. W., Szundi, I., Briggs, W. R., and Bogomolni, R. A. (2001) The photocycle of a flavin-binding domain of the blue light photoreceptor phototropin, *J. Biol. Chem. 276*, 36493−36500.
14. Corchnoy, S. B., Swartz, T. E., Lewis, J. W., Szundi, I., Briggs, W. R., and Bogomolni, R. A. (2003) Intermolecular proton transfers and structural changes during the photocycle of the LOV2 domain of phototropin 1, *J. Biol. Chem. 278*, 724−731.
15. Swartz, T. E., Wenzel, P. J., Corchnoy, S. B., Briggs, W. R., and Bogomolni, R. A. (2002) Vibration spectroscopy reveals light-induced choromophore and protein structural changes in the LOV2 domain of the plant blue-light receptor phototropin 1, *Biochemistry 41*, 7183−7189.
16. Abe, M., and Kyogoku, Y. (1987) Vibrational analysis of flavin derivatives: normal coordinate treatments of lumiflavin, *Spectrochim. Acta 43A*, 1027−1037.
17. Socrates, G. (2001) *Infrared and Raman Characteristic Group Frequencies*, Wiley, Chichester.
18. Wilde, A., Fiedler, B., and Börner, T. (2002) The cyanobacterial phytochrome Cph2 inhibits phototaxis towards blue light, *Mol. Microbiol. 44*, 981−988.
19. Ng, W.-O., Grossman, A. R., and Bhaya, D. (2003) Multiple light inputs control phototaxis in *Synechocystis* sp. strain 6803, *J. Bacteriol. 185*, 1599−1607.
20. Hellingwerf, K. J. (2002) The molecular basis of sensing and responding to light in microorganisms, *Antonie van Leeuwenhock 81*, 51−59.
21. Crosson, S., and Moffat, K. (2001) Structure of a flavin-binding plant photoreceptor domain: Insight into light-mediated signal transduction, *Proc. Natl. Acad. Sci. U.S.A. 98*, 2995−3000.
22. Crosson, S., and Moffat, K. (2002) Photoexcited structure of a plant photoreceptor domain reveals a light-driven molecular switch, *Plant Cell 14*, 1067−1075.
23. Salomon, M., Eisenreich, W., Dürr, H., Schleicher, E., Kneib, E., Massey, V., Rüdiger, W., Müller, F., Bacher, A., and Richter, G. (2001) An optomechanical transducer in the blue light receptor phototropin from *Avena sativa*, *Proc. Natl. Acad. Sci. U.S.A. 98*, 12357−12361.
24. Iwata, T., Tokutomi, S., and Kandori, H. (2002) Photoreaction of the cystein S−H group in the LOV2 domain of *Adiantum* phytochrome 3, *J. Am. Chem. Soc. 124*, 11840−11841.
25. Giovani, B., Byrdin, M., Ahmad, M., and Brettel, K. (2003) Light-induced electron transfer in a cryptochrome blue-light photoreceptor, *Nat. Struct. Biol. 10*, 489−490.
26. Abe, M., Kyogoku, Y., and Kitagawa, T. (1986) Infrared spectra and molecular association of lumiflavin and riboflavin derivatives, *Spectrochim. Acta 42A*, 1059−1068.
27. Nishina, Y., Sato, K., Miura, Retsu, Matsui, K., and Shiga, K. (1998) Resonance Raman study on reduced flavins in purple intermediate of flavoenzyme: use of [4-carbonyl-^{18}O]-enriched flavin, *J. Biochem. 124*, 200−208.
28. Iwata, T., Nozaki, D., Tokutomi, S., Kagawa, T., Wada, M., and Kandori, H. (2003) Light-induced structural changes in the LOV2 domain of *Adiantum* Phytochrome3 studied by low-temperature FTIR and UV−visible spectroscopy, *Biochemistry 42*, 8183−8191.
29. Lively, C. R., and McFarland, J. T. (1990) Assignment and the effect of hydrogen bonding on the vibrational normal modes of flavins and flavoproteins, *J. Phys. Chem. 94*, 3980−3994.
30. Hazekawa, I., Nishina, Y., Sato, K., Shichiri, M., Miura, R., and Shiga, K. (1997) A Raman study of the C(4)═O stretching mode of flavins in flavoproteins: hydrogen bonding at the C(4)═O moiety, *J. Biochem. 121*, 1147−1154.
31. Laan, W., van der Host, M. A., and Hellingwert, K. J. (2003) Initial characterization of the primary photochemistry of AppA, a blue-light-using flavin adenine dinucleotide-domain containing transcriptional antirepressor protein from *Rhodobacter sphaeroides*: A key role for reversible intramolecular proton transfer from the flavin adenine dinucleotide chromophore to a conserved tyrosine?, *Photochem. Photobiol. 78*, 290−297.
32. Pellet, J. D., Becker, D. F., Saenger, A. K., Fuchs, J. A., and Stankovich, M. T. (2001) Role of aromatic stacking interactions in the modulation of the two-electron reduction potentials of flavin and substrate/product in *Megasphaera elsdenii* short-chain acyl-Coenzyme A dehydrogenase, *Biochemistry 40*, 7720−7728.
33. Neiss, C., Saalfrank, P., Parac, M., and Grimme, S. (2003) Quantum chemical calculation of excited states of flavin-related molecules, *J. Phys. Chem. A 107*, 140−147.
34. Song, P.-S., Choi, J. D., Fugate, R. D., and Yagi, K. (1976) in *Flavins and Flavoproteins* (Singer, T. P., Ed.) pp 381−390, Elsevier, Amsterdam.
35. Nishimura, Y., and Tsuboi, M. (1978) Raman spectra of flavins: avoidance of interference from fluorescence, *Chem. Phys. Lett. 59*, 210−213.
36. Kitagawa, T., Nishina, Y., Kyogoku, Y., Yamano, T., Ohishi, N., Takai-Suzuki, A., and Yagi, K. (1979) Resonance Raman spectra of carbon-13- and nitrogen-15-labeled riboflavin bound to egg-white flavoprotein, *Biochemistry 18*, 1804−1808.
37. Nishima, Y., Shiga, K., Horiike, K., Tojo, H., Kasai, S., Yanase, K., Matsui, K., Watari, H., and Yamano, T. (1980) Vibrational modes of flavin bound to riboflavin binding protein from egg white, *J. Biochem. 88*, 403−409.
38. Copeland, R. A., and Spiro, T. G. (1986) Ultraviolet resonance Raman spectroscopy of flavin mononucleotide and flavin adenine dinucleotide, *J. Phys. Chem. 90*, 6648−6654.
39. Benecky, M., Li, T.-Y., Schmidt, J., Frerman, F., Watters, K. L., and McFarland, J. (1979) Resonance Raman study of flavins and the flavoprotein fatty acyl coenzyme a dehydrogenase, *Biochemistry 18*, 3471−3476.
40. Miura, R., Nishina, Y., Ohta, M., Tojo, H., Shiga, K., Watari, H., Yamano, T., and Miyake, Y. (1983) Resonance Raman study on the flavin in the purple intermediates of D-amino acid oxidase, *Biochem. Biophys. Res. Commun. 111*, 588−594.
41. Altose, M. D., Zheng, Y., Dong, J., Palfey, B. A., and Carey, P. R. (2001) Comparing protein−ligand interactions in solution and single crystals by Raman spectroscopy, *Proc. Natl. Acad. Sci. U.S.A. 98*, 3006−3011.
42. Ataka, K., Hegemann, P., and Heberie, J. (2003) Vibrational spectroscopy of an algal Phot-LOV1 domain probes the molecular changes associated with blue-light reception, *Biophys. J. 84*, 466−474.
43. Bowman, W. D., and Spiro, T. G. (1981) Normal-mode analysis of lumiflavin and interpretation of resonance Raman spectra of flavoproteins, *Biochemistry 20*, 3313−3318.
44. Kim, M., and Carey, P. R. (1993) Observation of a carbonyl feature for riboflavin bound to riboflavin-binding protein in the red-excited Raman spectrum, *J. Am. Chem. Soc. 115*, 7015−7016.
45. Hazekawa, I., Nishina, Y., Sato, K., Shichiri, M., Miura, R., and Shiga, K. (1997) A Raman study on the C(4)═O stretching mode of flavins in flavoenzymes: hydrogen bonding at the C(4)═O moiety, *J. Biochem. 121*, 1147−1154.
46. Harper, S. M., Neil, L. C., and Gardner, K. H. (2003) Structural basis of a phototropin light switch, *Science 301*, 1541−1544.

BI049836V